

# Atmospheric evolution of environmentally persistent free radicals in rural North China Plain: effects on water solubility and PM<sub>2.5</sub> oxidative potential

5 Xu Yang<sup>1</sup>, Fobang Liu<sup>1,\*</sup>, Shuqi Yang<sup>1</sup>, Yuling Yang<sup>2</sup>, Yanan Wang<sup>1</sup>, JingJing Li<sup>2</sup>, Mingyu Zhao<sup>2</sup>, Zhao Wang<sup>1,3</sup>, Kai Wang<sup>2</sup>, Chi He<sup>1</sup>, Haijie Tong<sup>4,\*</sup>

<sup>1</sup>Department of Environmental Science and Engineering, School of Energy and Power Engineering, Xi'an Jiaotong University, Xi'an, Shaanxi 710049, China

10 <sup>2</sup>State Key Laboratory of Nutrient Use and Management, College of Resources and Environmental Sciences, National Academy of Agriculture Green Development, National Observation and Research Station of Agriculture Green Development (Quzhou, Hebei), China Agricultural University, Beijing 100193, China

<sup>3</sup>Shaanxi Provincial Land Engineering Construction Group Co., Ltd., Xi'an, Shaanxi 710075, China.

<sup>4</sup>Institute of Surface Science, Helmholtz-Zentrum Hereon, Max-Planck-Str. 1, Geesthacht 21502, Germany

\*Corresponding authors: Fobang Liu ([fobang.liu@xjtu.edu.cn](mailto:fobang.liu@xjtu.edu.cn)); Haijie Tong ([haijie.tong@hereon.de](mailto:haijie.tong@hereon.de))

## Abstract

15 Environmentally Persistent Free Radicals (EPFRs) represent a novel class of hazardous substances, posing risks to human health and the environment. In this study, we investigated the EPFRs in ambient fine, coarse, and total suspended particulate matter (PM<sub>2.5</sub>, PM<sub>10</sub>, TSP) in rural North China Plain, where local primary emissions of EPFRs were limited. We observed that the majority of EPFRs occurred in PM<sub>2.5</sub>. Moreover, distinct seasonal patterns and higher g-factors of EPFRs were found compared to those in urban environments, suggesting unique characteristics of EPFRs in rural areas. The source apportionment  
20 analyses revealed atmospheric oxidation as the largest contributor (33.6%) to EPFRs. A large water-soluble fraction (35.2%) of EPFRs was determined, potentially resulting from the formation of more oxidized EPFRs through atmospheric oxidation processes during long-range/regional transport. Additionally, significant positive correlations were observed between EPFRs and the oxidative potential of water-soluble PM<sub>2.5</sub> measured by dithiothreitol-depletion and hydroxyl-generation assays, likely

attributable to the water-soluble fractions of EPFRs. Overall, our findings reveal the prevalence of water-soluble EPFRs in rural areas and underscore atmospheric oxidation processes can modify their properties, such as increasing their water solubility. This evolution may alter their roles in contributing to the oxidative potential of PM<sub>2.5</sub> and potentially also influence their impact on climate-related cloud chemistry.

## 1. Introduction

Environmentally persistent free radicals (EPFRs) are a new class of risk substances that have garnered significant attention in recent years (Yi et al., 2023; Vejerano et al., 2018). Unlike short-lived radicals, EPFRs are characterized by their stability, with lifetimes ranging from days to months, and even indefinite (Gehling and Dellinger, 2013; Runberg et al., 2020). They have been identified in various environmental matrices, including soil, sediment, leaves, industrial fly ash, household dust, and atmospheric particulate matter (PM) (Jia et al., 2017; Vejerano and Ahn, 2023; Zhao et al., 2019b; Filippi et al., 2022; Arangio et al., 2016). Of particular interest is their presence in inhalable atmospheric PM, which serves as a crucial carrier for EPFRs, amplifying their detrimental health impacts. Toxicological studies have demonstrated that EPFRs can induce lung damage by triggering oxidative stress in lung cells, primarily through the reactive oxygen species (ROS) generated from the catalytic cycling of EPFRs (Wang et al., 2011; Balakrishna et al., 2009; Yi et al., 2023). Moreover, the persistent nature of EPFRs and their activation potential by certain environmental factors (e.g., water molecules and ultraviolet light) enable them to participate in diverse atmospheric reactions, initiating or propagating subsequent radical reactions (Truong et al., 2010; Sarmiento and Majestic, 2023; Comandini et al., 2012). Thus, understanding the sources and properties of EPFRs is essential for assessing their atmospheric and health impacts.

The occurrence of EPFRs was initially detected in aerosols originating from cigarette smoke (Pryor et al., 1983), and later also in combustion-derived particles as well as ambient PM (Dalal et al., 1991). Various combustion and thermal processes

including industrial processes, coal combustion, biomass burning, engine exhaust, and waste incineration, have been identified  
45 as important sources of EPFRs (Liu et al., 2021; Yang et al., 2017; Wang et al., 2020a). Mechanistic studies suggest that EPFRs  
can be generated and stabilized on the surfaces of transition metal-doped particles in the post-flame and cool-zone regions of  
combustion systems (Cormier et al., 2006). In addition, secondary chemical processes of organic molecules, may also  
contribute to the presence of EPFRs in atmospheric PM (Chen et al., 2019; Wang et al., 2020a). Previous work has shown that  
EPFRs can be formed through the oxidation of organic molecules by ozone and photochemical reactions of PM (Borrowman  
50 et al., 2016; Sarmiento and Majestic, 2023; Qin et al., 2021; Tong et al., 2018). Various factors, including solar irradiation,  
humidity, and the types of precursors, may influence the formation of secondary EPFRs (Sarmiento and Majestic, 2023; Chen  
et al., 2019; Liu et al., 2023).

Multiple studies conducted in recent decades have investigated the composition of EPFRs in atmospheric PM (Yang et  
al., 2017; Arangio et al., 2016; Xu et al., 2020). The identified types of EPFRs include carbon-centered and oxygen-centered  
55 free radicals, as well as carbon-centered free radicals with a nearby heteroatom. These radicals often manifest as  
cyclopentadienyl, semiquinone, and phenoxy radicals (Ai et al., 2023). Notably, Chen et al. (2018b) revealed that the dominant  
fraction of EPFRs existed within nonsolvent-extractable (unable to be extracted by water, methanol, dichloromethane, and n-  
hexane) organic matter of urban PM<sub>2.5</sub>, underscoring the need for further exploration into the organic molecules associated  
with ambient EPFRs.

60 EPFRs exhibit redox activity, capable of reducing oxygen and facilitating the formation of ROS such as hydroxyl radicals  
(•OH) and superoxide radicals (O<sub>2</sub>•) (Hwang et al., 2021; Guo et al., 2020). Consequently, EPFRs may serve as crucial  
hazardous components contributing to the toxicity of atmospheric PM. Li et al. (2023) found that EPFRs can contribute to the  
oxidative toxicity of both water-soluble and -insoluble fractions of atmospheric PM. The types of EPFRs and their extractability  
may influence their roles in ROS formation (Zhao et al., 2019b). Moreover, ambient EPFRs have been detected in both fine

65 and coarse particles, with observed seasonal and spatial variations in their size distribution (Jia et al., 2023; Wang et al., 2022).  
The presence of EPFRs in different particle sizes may pose various health risks to humans due to differences in deposition  
efficiency within the respiratory tract.

The investigations of airborne EPFRs in urban areas, heavily influenced by traffic, industrial, and residential emissions,  
have been the primary focus of previous studies (Yang et al., 2017; Wang et al., 2020a). However, EPFRs, characterized by  
70 their long lifetimes, can undergo transport over considerable distances and reach rural areas with minimal local emissions.  
Indeed, the long-range transport of EPFRs has been demonstrated (Chen et al., 2018a). During the transport, the characteristics  
of EPFRs may undergo evolution through atmospheric chemical processes, potentially altering their roles in ROS formation.  
Despite this, investigations into the characteristics of airborne EPFRs in areas with limited local emissions remain sparse.  
Insights into airborne EPFRs in such areas will allow a better understanding of the atmospheric transformation and fate of  
75 EPFRs as well as their atmospheric and health effects.

Therefore, to enhance our understanding of EPFR evolution during atmospheric transport and its effects on ROS  
formation by the corresponding PM, we collected yearlong PM samples in a typical rural area located in the North China Plain  
(NCP), where local combustion emissions contributing to EPFRs are minimal. On the other hand, northern China, including  
NCP, is one of the most polluted regions in China, characterized by significant combustion sources, making the selected  
80 location ideal for our research objectives. Specifically, our study aims to (i) investigate the characteristics of EPFRs, including  
their concentration, size distribution, and seasonal variations in the studied region; (ii) determine the sources of EPFRs; (iii)  
explore the roles of EPFRs' speciation in contributing to the oxidative potential of PM.

## **2. Methods**

### **2.1 PM sample collection**

85 Ambient PM samples were collected at a rural site (36°51'48"N 115°00'58"E) in Quzhou county in the NCP from April  
2022 to March 2023. The sampling site represents a typical rural environment, predominantly surrounded by croplands and  
devoid of significant local industrial sources (Figure S1). Sequential 24-hour fine (PM<sub>2.5</sub>), coarse (PM<sub>10</sub>), and total suspended  
particles (TSP) were collected using a high-volume sampler (TH-1000CII, Tianhong, China) at a flow rate of 1.05 m<sup>3</sup>/min.  
The PM samples were collected onto prebaked (900 °C) quartz filters (Munktell, type MK360) and stored at -20 °C until  
90 analysis. In total, ninety-five PM samples were collected during the whole sampling. A summary of the number of PM<sub>2.5</sub>, PM<sub>10</sub>,  
and TSP samples collected in each season is provided in Table S1. In addition, other air quality parameters (SO<sub>2</sub>, NO<sub>2</sub>, O<sub>3</sub>, and  
CO) data were obtained from the monitoring site nearest to the sampling site from the local environmental monitoring center.

## 2.2. EPFRs analysis

Three punches (1.2 cm<sup>2</sup> per punch) of each filter were inserted into a quartz tube (5 mm I.D., SP Wilmad-LabGlass) for  
95 EPFR measurements using an EPR spectrometer (A300-9.5/12, Bruker). The detection parameters for EPFRs were set as  
follows: a modulation frequency of 100 kHz; a microwave frequency of 9.8485 GHz; a microwave power of 1.76 mW; a  
modulation amplitude of 1.00 G; a sweep width of 150 G; a time constant of 81.92 ms; a receiver gain of  $1 \times 10^3$  G. All EPR  
measurements were conducted at room temperature. To minimize noise in EPR signals, a baseline correction was performed,  
followed by fitting the signals using a Gaussian function via the least squares method. EPFR concentrations for the filters were  
100 determined by comparing the peak area with a calibration curve (Figure S2) generated using a common radical stand, 4-  
hydroxy-2,2,6,6-tetramethylpiperidin-1-oxyl (TEMPOL) (Arangio et al., 2016).

In addition, we conducted water extraction and acidification experiments on the samples to determine the reduction of  
EPFR contents on the filter samples after treatment. The procedures of water extraction and acidification were adopted from  
previous studies (Chen et al., 2018b; Yang et al., 2017). For water extraction, all PM<sub>2.5</sub> samples were processed alongside two  
105 randomly selected PM<sub>10</sub> and TSP samples from each season. Briefly, three punches (1.2 cm<sup>2</sup> per punch) of each filter were

immersed in 3 mL of deionized water for 14 hours under dark condition. Regarding acidification, two PM<sub>2.5</sub>, PM<sub>10</sub>, and TSP samples in each season were randomly selected, and two punches (1.2 cm<sup>2</sup> per punch) of each filter were immersed in 2 mL of 6 M HCl solution for one hour under dark condition. Subsequently, the filter punches were dried by a vacuum freeze dryer before conducting EPFRs measurements using the aforementioned detection parameters. All the EPFR measurements were conducted within one year after sampling.

### 2.3 Carbonaceous fractions and element analyses

A 1.0 cm<sup>2</sup> punch of each sample filter was analyzed for organic carbon (OC) and elemental carbon (EC) following the Interagency Monitoring of Protected Visual Environments (IMPROVE) thermal/optical reflectance (TOR) protocol using the DRI Model 2001 carbon analyzer. Different carbonaceous fractions, including OC1–4 and EC1–3, were isolated and quantified based on their thermal stability.

Twelve elements (Li, Mg, Al, Si, K, Ca, Cr, Mn, Fe, Cu, Zn, and Pb) were analyzed using inductively coupled plasma mass spectrometry (ICP-MS, Thermo Scientific iCAP RQ). Prior to analysis, a 3.6 cm<sup>2</sup> punch of each filter was digested using 1 mL of aqua regia (HNO<sub>3</sub>+3HCl, v:v) at 99 °C and a rotational frequency of 350 rpm for 24 hours. After digestion, the extracts were filtered through a 0.22 µm PTFE syringe filter and then diluted to 5 mL deionized water with 2% HNO<sub>3</sub>.

### 2.4 Oxidative potential measurements

The oxidative potential of PM samples was measured by two techniques, the dithiothreitol (DTT) depletion assay and •OH production assay (Verma et al., 2012; Son et al., 2015). In the DTT assay, the decay of 100 µM DTT by PM in phosphate buffer was monitored over a 40-minute incubation at 37 °C. The remaining DTT after the incubation was quantified by its reaction with dithiodinitrobenzoic acid, yielding ultraviolet-detectable 2-nitro-5-thiobenzoic acid (Verma et al., 2012; Fang et al., 2015). In the •OH production assay, the terephthalate (10 mM) in phosphate buffer was used to measure •OH radical

formation by PM throughout 2-hour incubation at 37 °C. At pH 7.4, terephthalate reacted with •OH to form stable and highly fluorescent hydroxyterephthalic acid (2-OHTA), and the production rate of •OH was calculated based on the produced 2-OHTA, as the formation of 2-OHTA is proportional to the generation of •OH (Yu et al., 2022; Li et al., 2019). Note that samples were incubated at a PM concentration of 100 µg/mL for both assays. Meanwhile, both total OP (Total-OP) and water-soluble OP (WS-OP) were determined in this work. For total OP determination, unfiltered PM extracts with filter punches left in the extracts were directly incubated with the probes. While for water-soluble OP, the extract was filtered through a 0.22 µm PTFE syringe filter before incubating with probes. The OP contribution from water-insoluble PM components (water-insoluble OP, WIS-OP) was considered as the difference between Total-OP and WS-OP. A detailed description of the DTT and •OH assays can be found in the Supporting Information (Text S1).

## 2.5 Statistical analysis

### 2.5.1 Positive matrix factorization

The EPA positive matrix factorization (PMF 5.0) model was employed to apportion the sources of EPFRs and PM in this study. The PMF model is an advanced multivariate factor analysis tool widely utilized for source apportionment of environmental pollutants (Heo et al., 2013; Wang et al., 2019). The input data include the concentrations and uncertainties of PM, EPFRs, organic carbon fractions (OC1, OC2, OC3), elemental carbon fractions (EC1, EC2, EC3), SO<sub>2</sub>, NO<sub>2</sub>, CO, O<sub>3</sub>, and the twelve elements. The uncertainties of each variable were calculated using the equation: Uncertainty = K × Concentration, where K denotes analytical uncertainty (Wang et al., 2019). For PM, EPFRs, OC, and EC, K was set as 10% (Jang et al., 2020). For metal elements and meteorological parameters, K was set as 15% (Ikemori et al., 2021). Missing values and associated uncertainties were estimated by substituting the median concentrations of the components and four times the median value of the components to mitigate their impact on the results (Wang et al., 2019).

The PMF model was run with four to seven factors and with random seeds. The six-factor result was considered as the

optimal one based on minimal Q value (indicating the variation between observation and the model is the least),  $Q_{\text{Robust}}/Q_{\text{Theo}}$  ( $< 2$ ), scaled residuals (within  $\pm 3$ ), and the interpretable profiles from the literature (Reff et al., 2007; Ramadan et al., 2000). Bootstrap and displacement analyses were conducted to estimate the uncertainty of the PMF model with six factors (Brown et al., 2015), and the results are shown in Figure S3. The bootstrap factor mapping exceeded 93% for all factors without any displacement run exchanges.

### 2.5.2 Correlation analysis

Correlation analysis was performed using Pearson's correlation coefficients and two-tailed significance tests by IBM SPSS Statistics 27.

### 2.6 Backward trajectories

To characterize the origins and transport pathways of the air masses to the sampling site, 48-h backward trajectories of the air masses were simulated using the Hybrid Single Particle Lagrangian Integrated Trajectory (HYSPPLIT) model. The input meteorological data were acquired from the Global Data Assimilation System (<ftp://arlftp.arlhq.noaa.gov/pub/archives/gdas1>).

## 3. Results and discussion

### 3.1 Characteristics of EPFRs in different sizes of PM

Figure 1a illustrates the box plots of volume-normalized (EPFR<sub>v</sub>) concentrations of EPFRs in different sizes of PM during the entire sampling. EPFR<sub>v</sub> levels in PM<sub>2.5</sub>, averaging  $(5.6 \pm 1.1) \times 10^{12}$  spins/m<sup>3</sup>, accounted for over 95.2% of those in PM<sub>10</sub> ( $(5.8 \pm 1.0) \times 10^{12}$  spins/m<sup>3</sup>) and TSP ( $(5.9 \pm 1.1) \times 10^{12}$  spins/m<sup>3</sup>). However, the average mass concentration of PM<sub>2.5</sub> only represented 61.8% of that in PM<sub>10</sub>, and 47.5% of that in TSP (Figure S4). Similar results were found for EPFR<sub>v</sub> and PM concentrations in each season (Figure S5). These results suggest that the majority of airborne EPFRs are present in PM<sub>2.5</sub>, with



only a small portion occurring in the 2.5-10  $\mu\text{m}$  size range.

This is further evident by the results of mass-normalized (EPFR<sub>m</sub>) concentration of EPFRs, as depicted in Figure 1b. The average EPFR<sub>m</sub> in PM<sub>2.5</sub> ( $6.5 \pm 3.5$ )  $\times 10^{16}$  spins/g) was approximately 1.7 times that in PM<sub>10</sub> ( $(3.9 \pm 2.1) \times 10^{16}$  spins/g), and 2.2 times that in TSP ( $(3.0 \pm 1.7) \times 10^{16}$  spins/g). Consistent with our finding, previous studies have also observed a predominant fraction of EPFRs in smaller sizes (< 2.5  $\mu\text{m}$ ) of PM (Chen et al., 2020; Dugas et al., 2016). The strong association of EPFRs with fine particles may stem from multiple factors. Firstly, airborne EPFRs primarily originate from the combustion of organic materials and multiphase chemistry of gaseous organics in the atmosphere, processes that predominantly form fine particles (Tian et al., 2009; Arangio et al., 2016). Additionally, the larger specific surface area and porous structure of fine particles facilitate the attachment of EPFRs, leading to their higher retention within this fraction (Yang et al., 2017).

Table S2 presents a summary of the concentrations of EPFR<sub>v</sub> and EPFR<sub>m</sub> in this study compared to existing literature. Both EPFR<sub>v</sub> and EPFR<sub>m</sub> in this study were lower than in most urban and suburban environments (Wang et al., 2019; Jia et al., 2023; Yang et al., 2017). This implies that there were only limited local sources directly emitting EPFRs at this rural site. This is further supported by the seasonal variation of EPFRs. Notably, higher EPFR<sub>v</sub> levels were observed in summer than in winter (Figure 1c), with the highest EPFR<sub>m</sub> occurring during summer (Figure 1d) in the studied area. This contrasts with findings from previous studies, which indicated that winter typically exhibits the highest EPFR<sub>v</sub>, especially for cities in northern China with prominent local emission sources of EPFRs, such as large-scale coal consumption (Wang et al., 2019; Jia et al., 2023; Ai et al., 2023). The distinct seasonal characteristic of EPFRs observed in our study could be attributed to the limited residential and industrial activities in rural NCP. On the other hand, the highest EPFR<sub>m</sub> levels in summer may be linked to enhanced atmospheric oxidation, promoting EPFR formation due to elevated concentrations of photo-oxidants and stronger solar irradiation (Borrowman et al., 2016; Sarmiento and Majestic, 2023; Shiraiwa et al., 2011).

In addition to examining the concentrations of EPFRs, we also investigated the g-factors of EPFRs across different sizes

of PM, as the g-factor is an important indicator of EPFRs characteristics. We observed that the g-factors for all PM samples ranged between 2.0033 and 2.0037, with a mean value of  $2.0035 \pm 0.0001$  (Figure S6). These g factors are higher than the values obtained from PM samples collected from highway and urban locations (Hwang et al., 2021; Fang et al., 2023). A g-factor below 2.003 signifies the presence of carbon-centered radicals (e.g., cyclopentadienyl), while a g-factor exceeding 2.004 indicates oxygen-centered radicals (e.g., phenoxy, semiquinone radicals). A g factor falling between 2.003–2.004 suggests a carbon-centered radical with adjacent oxygen atoms (Ai et al., 2023; Yang et al., 2017). The observed g factors in this work indicate the presence of carbon-centered radicals with adjacent oxygen atoms and oxygen-centered radicals. Furthermore, we noted a decreasing trend in the g-factor with particle size (i.e.,  $PM_{2.5} > PM_{10} > TSP$ ), indicating closer proximity of the unpaired electron to the oxygen center in smaller particles. This trend could be attributed to the increased exposure of porous structures in smaller particles, rendering them more susceptible to oxidation (Yang et al., 2017).

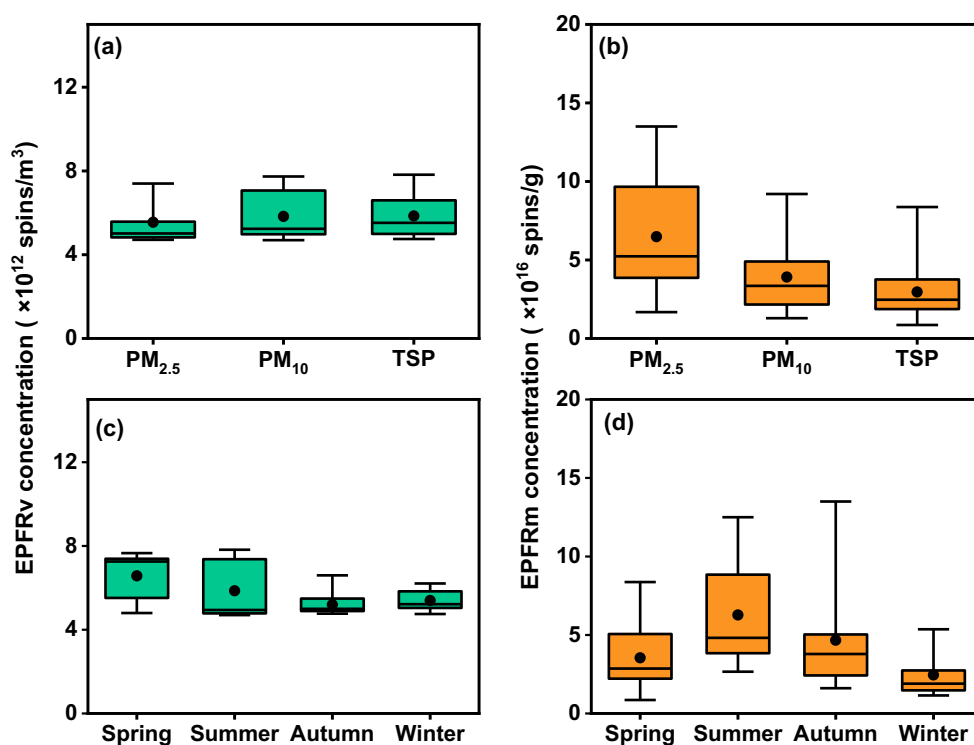


**Figure 1.** The concentrations of EPFR<sub>v</sub> (a and c) and EPFR<sub>m</sub> (b and d) in different sizes of PM samples and different seasons. The boxes represent the 25<sup>th</sup> percentile (lower edge), median (solid line), mean (solid dot), and 75<sup>th</sup> percentile (upper edge). The whiskers represent the minimum and maximum.

### 3.2 Sources of EPFRs

The PMF analysis was utilized to identify and quantify the sources contributing to EPFRs. As shown in Figure 2a, six primary source factors were determined. Factor 1 was attributed to atmospheric oxidation, characterized by its elevated proportion of O<sub>3</sub>. The presence of O<sub>3</sub> signifies atmospheric oxidative capability (Ainur et al., 2023; Wang et al., 2020b). Factor 2 exhibited high proportions of Al, Fe, Cr, SO<sub>2</sub>, CO, and EC, suggesting industrial emissions. Al and Fe could be associated with iron and steel production and the metal industry (Khobragade and Ahirwar, 2022). The availability of Cr is linked to fossil fuel combustion or oil combustion (Alleman et al., 2010; Begum et al., 2011). SO<sub>2</sub> and CO are typical tracers of coal combustion (Johnson et al., 2006; Kundu et al., 2010; Wang et al., 2019), and they (and also EC) could be emitted from coal-based industries. Factor 3, characterized by high proportions of SO<sub>2</sub>, NO<sub>2</sub>, and CO, was identified as coal combustion (Johnson et al., 2006; Kundu et al., 2010; Wang et al., 2019). Previous research indicates that NO<sub>2</sub> emissions, although often associated with vehicle emissions, are also prevalent in coal combustion (Ainur et al., 2023; Lei et al., 2016; Wang et al., 2018a). In factor 4, high proportions of OC<sub>3</sub>, OC<sub>4</sub>, EC<sub>1</sub>, EC<sub>2</sub>, EC<sub>3</sub>, Mn, Cu, and Pb were observed, suggesting motor vehicle emissions. EC<sub>1</sub>, OC<sub>2</sub>, OC<sub>3</sub>, and OC<sub>4</sub> primarily originate from petrol vehicle emissions, while EC<sub>2</sub> and EC<sub>3</sub> are closely associated with diesel vehicle emissions (Kim and Hopke, 2004; Ai et al., 2023). Additionally, Mn (from unleaded gasoline additives), Pb (from gasoline additives), and Cu (from brake linings) contribute to this factor (Sharma et al., 2014). Factor 5 displayed a high loading of OC<sub>1</sub> and a considerable loading of OC<sub>2</sub>, indicative of biomass burning. OC<sub>1</sub> and OC<sub>2</sub> have been linked to biomass combustion in previous studies (Stanimirova et al., 2023; Cao et al., 2005; Dong et al., 2022). Factor 6 exhibited high proportions of Mg and Ca, suggesting soil dust as these elements are major constituents of the Earth's crust (An et al., 2015; Liu et al., 2022b).

220 In summary, the six primary sources contributing to EPFRs were identified as atmospheric oxidation, industrial emissions, coal combustion, motor vehicle emissions, biomass burning, and soil dust. As shown in Figure 2b, atmospheric oxidation emerged as the largest contributor (33.6%) to EPFRs during the entire sampling period. The formation of EPFRs through atmospheric oxidation could occur via photo-oxidant oxidation (reactions of polycyclic aromatic hydrocarbons (PAHs) with solar radiation, O<sub>3</sub> and •OH) and metal-catalyzed redox reaction (PAHs interacting with metals under visible and UV light irradiation). Solar radiation and O<sub>3</sub> can directly generate EPFRs by disrupting the stable covalent bonds of organic substances, while metals act as electron acceptors, facilitating electron transfer with PAHs to form EPFRs, as suggested by previous studies (Borrowman et al., 2016; Shiraiwa et al., 2011; Chen et al., 2019; Wang et al., 2020a).

230 The significant contribution of atmospheric oxidation observed in our study contrasts with findings from urban areas, where primary sources typically dominate airborne EPFRs (Ainur et al., 2023; Ainur et al., 2022). The results of seasonal source apportionments (Figure 2b) further illustrate much higher contributions of atmospheric oxidation in spring (42.2%) and summer (50.3%) compared to autumn (21.3%) and winter (18.6%). The elevated contribution in summer aligned with the expectation of stronger photochemistry. The relatively high contribution in spring could be attributed to the dominance of long-range transport of air mass (60%, Figure S7a), which was markedly higher than the proportions (< 23%) observed in the other seasons. Previous studies have suggested that long-range transport of air mass favors atmospheric oxidation occurrence more than the air mass from regional/short-range transport (Ramya et al., 2023; Zhong et al., 2022).

240 Industrial emissions (30.8%) were the second largest contributor to annual EPFRs, followed by coal combustion (14.5%), motor vehicle emissions (10.3%), biomass burning (6.6%), and soil dust (4.2%). Industrial emissions and coal combustion have been widely suggested as significant sources of EPFRs (Wang et al., 2020a; Yang et al., 2017; Wang et al., 2018b). Although industrial activities were limited at this rural site, emissions might originate from surrounding industrial cities such as Handan in the south, as indicated by backward trajectory analysis (Figure S7). Over 17% of air mass was identified as

regional transport from the south, particularly notable in autumn (54%), corresponding to a higher contribution (44.7%) of industrial emissions to EPFRs compared to other seasons. Winter exhibited notably higher contributions from coal combustion and biomass burning, as coal and biomass are primary fuels for residential heating in rural NCP during this season.

245 While motor vehicle emissions accounted for a small contribution to EPFRs, they constituted the largest contributor (43.8%) to PM (Figure S8), suggesting differing components contribute to EPFRs and PM. For instance, volatile organic compounds (e.g., toluene) and nitrogen oxides emitted from vehicle exhausts may significantly contribute to PM formation but are generally not considered as major contributors to EPFRs (Nagpure et al., 2016; Gao et al., 2022; Wang et al., 2019). Regarding soil dust, recent studies indicate that PAHs readily adsorb on mineral surfaces, likely forming “cation- $\pi$ ” interactions with active sites. This interaction promotes electron transfer from aromatic compounds to surface cations on clay surfaces, 250 facilitating the formation of intermediate radicals/final products (Zhao et al., 2019a; Ni et al., 2023).

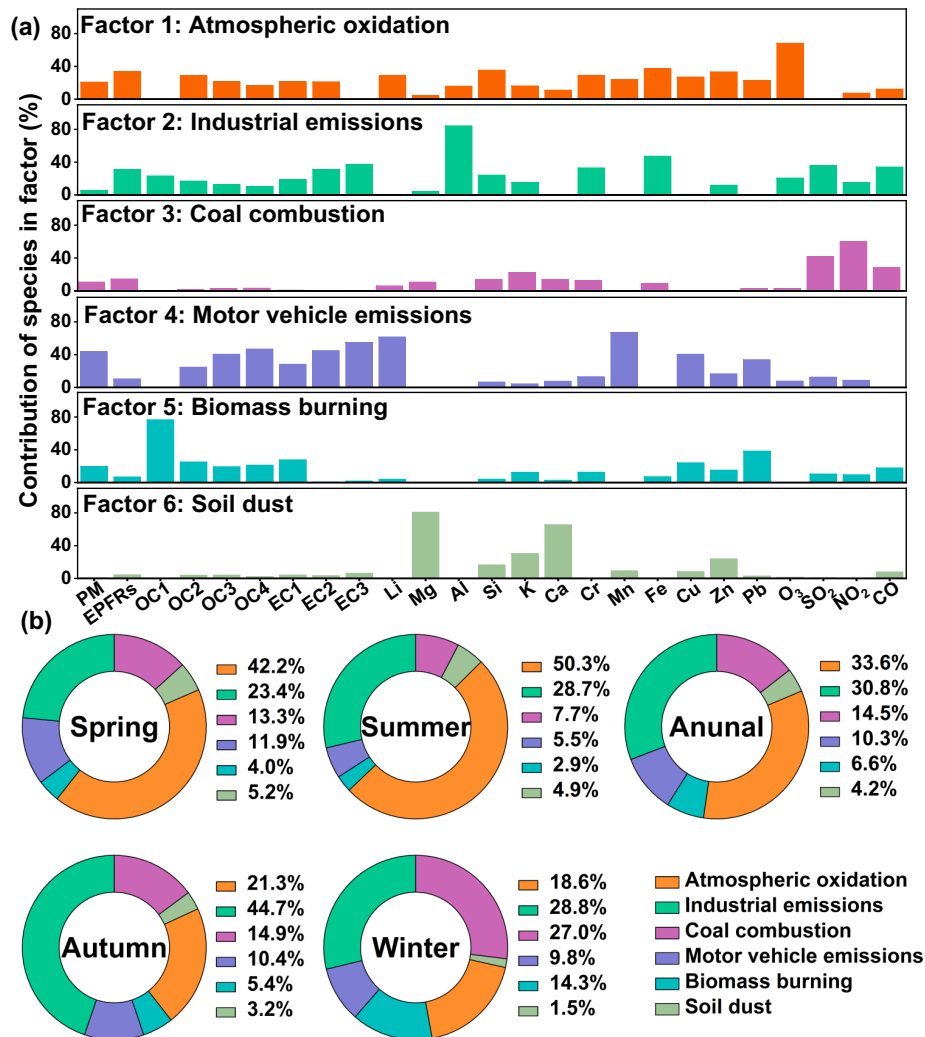


**Figure 2.** (a) Factor profile obtained by positive matrix factorization analysis. (b) Seasonal and annual contributions of the six factors to EPFRs.

### 3.3 Associations of EPFRs with OP of PM

#### 255 3.3.1 OP of PM

Oxidative potential, defined as the catalytic generation of ROS by PM components, serves as a plausible metric for assessing PM toxicity (Abrams et al., 2017; Weichenthal et al., 2016; Daellenbach et al., 2020; Bhattu et al., 2024). EPFRs have been identified as significant contributors to the OP of PM due to their ability to catalytically generate ROS (Gehling et

al., 2014; Hwang et al., 2021). In this work, we also measured the OP of the PM samples using two commonly used assays:  
260 dithiothreitol-depletion ( $OP^{DTT}$ ) and hydroxyl-generation ( $OP^{OH}$ ) assays.  $OP^{DTT}$  is found to be a good indicator of the  
production of  $O_2^-$  and  $H_2O_2$  but does not capture  $\bullet OH$  generation (Fang et al., 2019). Thus, the combined application of two  
assays provides complementary insights into the role of EPFRs in ROS generation. Further, WS-OP, WIS-OP, and Total-OP  
were all determined to explore their potential correlations with EPFRs.

Tables S3 and S4 summarize the OP results in this work. A detailed discussion of OP values between the present work  
265 and literature can also be seen in the Supporting Information (Text S2). In short, consistent with the findings of EPFRm, the  
OPm values in this work were also lower than in most urban and suburban environments. This disparity suggests fewer redox-  
active PM components in the studied rural area, likely due to the absence of significant local emission sources of pollutants.

Figure 3a illustrates the box plots of mass-normalized WS-OP, WIS-OP, and Total-OP determined by the two assays.  
Generally, Total-OP levels were higher than WS-OP and WIS-OP, demonstrating measurable contributions of both water-  
270 soluble and -insoluble species to the overall OP of PM. Additionally, WS-OP accounted for a larger fraction of Total-OP in  
both assays ( $WS-OP^{DTT}$ :  $67.8 \pm 20.5\%$ ;  $WS-OP^{OH}$ :  $56.1 \pm 22.6\%$ ). Furthermore, a reverse relationship between particle size  
and the contribution of WS-OP to Total-OP was observed, with the largest contribution in  $PM_{2.5}$ , followed by  $PM_{10}$  and TSP  
(Figure 3b). A significantly higher contribution of  $WS-OP^{DTT}$  to  $Total-OP^{DTT}$  has also been observed for ambient  $PM_{2.5}$  at  
multiple locations worldwide (Gao et al., 2017; Yang et al., 2024; Li et al., 2024). Yet, PM samples near highways and road  
275 dust have shown a higher fraction of  $WIS-OP^{DTT}$  than  $WS-OP^{DTT}$  (Zhang et al., 2024; Li et al., 2023). This could be due to a  
lower solubility of PM at the sites near primary emissions. These divergent results suggest that atmospheric oxidation processes  
may alter the role of PM components in contributing to OP.

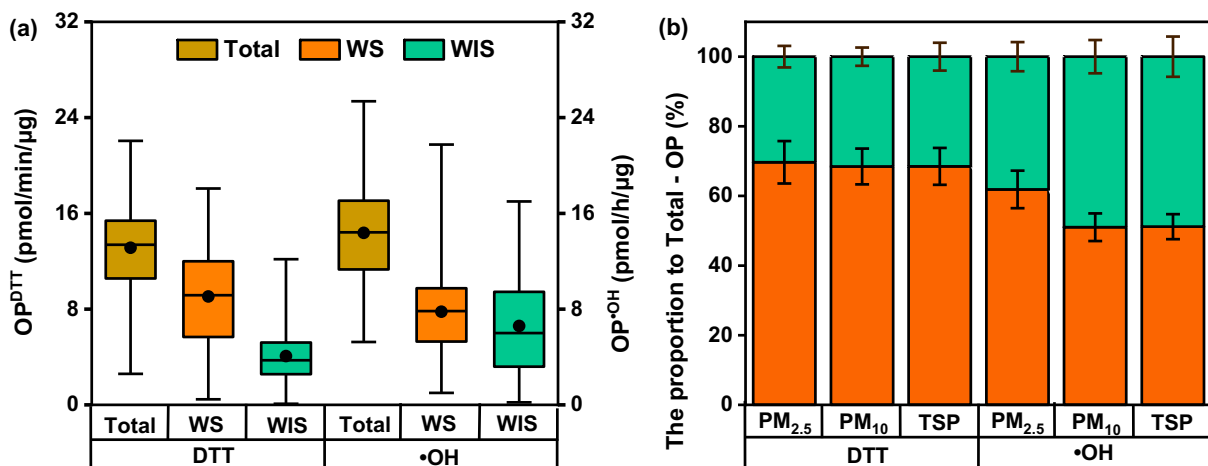


**Figure 3.** (a) The concentrations of total, water-soluble (WS), water-insoluble (WIS) fractions of OP<sup>DTT</sup> and OP<sup>•OH</sup>. The boxes represent the 25<sup>th</sup> percentile (lower edge), median (solid line), mean (solid dot), and 75<sup>th</sup> percentile (upper edge). The whiskers represent the minimum and maximum. (b) Proportions of WS-OP and WIS-OP to Total-OP in different sizes of PM samples and the bar indicates the standard error.

### 3.3.2 Associations among EPFRs, OP, and PM components

To identify individual chemical species influencing the intrinsic redox activity of ambient PM, correlation analyses between mass-normalized OP (OP<sup>DTT/•OH</sup>) and the mass fraction of determined chemical species, were performed. The results are shown in Figure 4 and the detailed information is also listed in Tables S5–7 (the volume-normalized correlation results are also included in Figure S9 in case the readers are interested).

Notably, the chemical species associated with Total-OP and WS-OP exhibited similarities, particularly for PM<sub>2.5</sub> (Figure 4). This may be partly because Total-OP was primarily comprised of WS-OP (Figure 3b). Also, good correlations were observed between Total-OP and WS-OP, except for the OP<sup>•OH</sup> of TSP samples (Figure S10). In addition, we observed that OP<sup>DTT</sup> and OP<sup>•OH</sup> were sensitive to different chemical species (Figure 4). Specifically, OC, EC, EPFRs, Fe, and Cr showed good correlations with Total-OP<sup>DTT</sup> and WS-OP<sup>DTT</sup>; while Cu exhibited a good correlation with Total-OP<sup>•OH</sup> and WS-OP<sup>•OH</sup> ( $r > 0.5$ ,  $p < 0.05$ ). As aforementioned, OP<sup>DTT</sup> is a good indicator of the production of O<sub>2</sub><sup>-</sup> and H<sub>2</sub>O<sub>2</sub> (Fang et al., 2019). Thus, these results indicate that different chemical species contribute to the production of distinct types of ROS (Campbell et al.,



2021; Jin et al., 2019; Calas et al., 2018). In terms of WIS-OP, only OC showed a moderate correlation ( $r = 0.43$ ,  $p < 0.05$ )  
295 with WIS-OP<sup>DTT</sup>. No species displayed a positively good correlation with WIS-OP<sup>OH</sup>, implying that WIS-OP might arise from  
complex synergistic/antagonistic interactions among PM components (Charrier and Anastasio, 2015; Yu et al., 2018). However,  
further research is warranted to elucidate the mechanisms and PM components responsible for WIS-OP.

Interestingly, EPFRs in PM<sub>2.5</sub> exhibited significant correlations with WS-OP but not with WIS-OP (Figure 4). This  
observation contradicts previous studies reporting that the majority of EPFRs are not water-extractable (Chen et al., 2018b;  
300 Guo et al., 2023; Wang et al., 2018b). Given the source apportionment results showing atmospheric oxidation as the largest  
contributor to EPFRs, we hypothesized that atmospheric oxidation processes may have increased the water solubility of rural  
EPFRs, leading to the observed significant correlations.

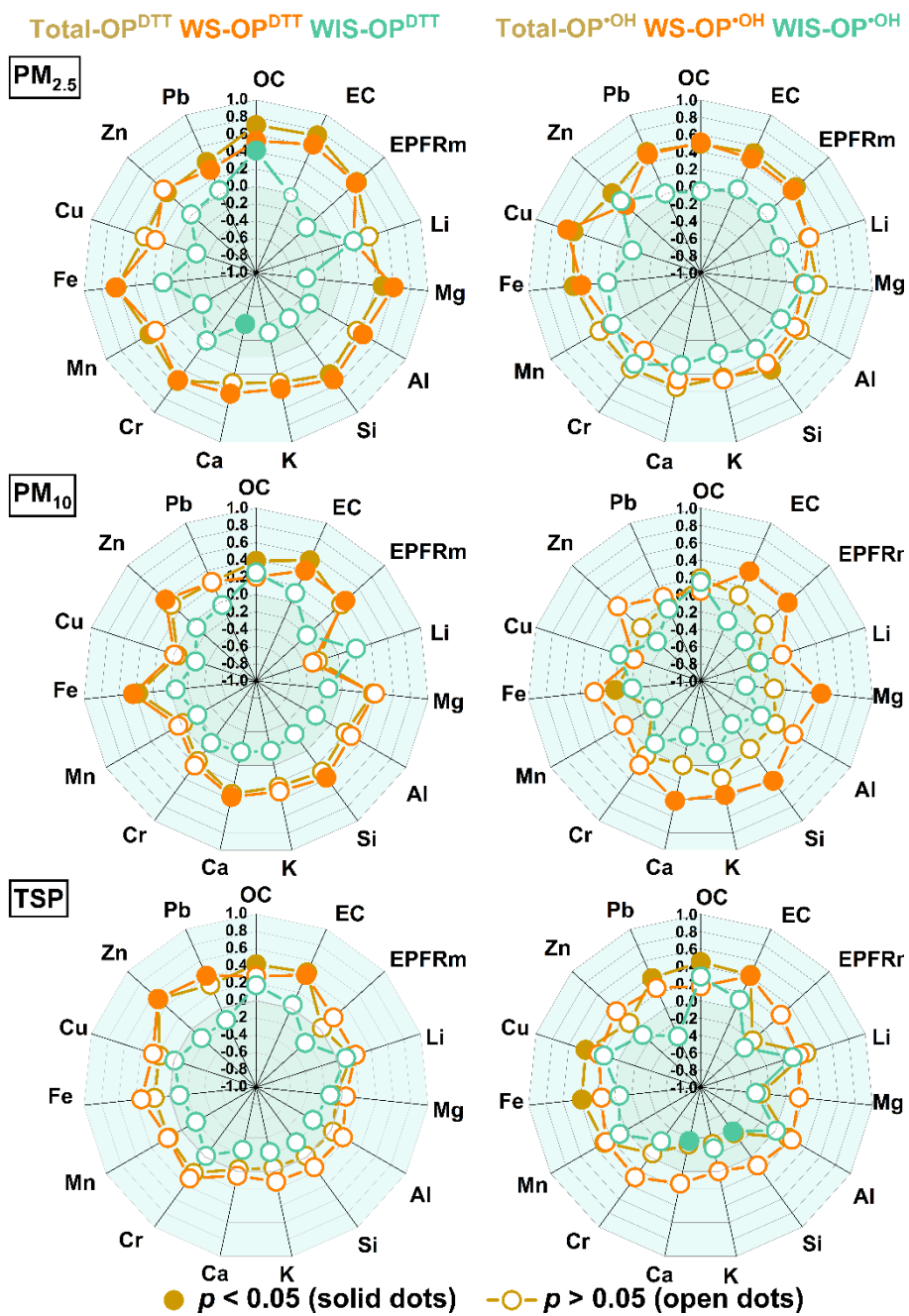


**Figure 4.** Correlation coefficients (Pearson's  $r$ ) of mass-normalized OP (Total/WS/WIS) with mass fractions of selected chemical species.

### 305 3.3.3 Solubility of EPFRs and its linkages with OP

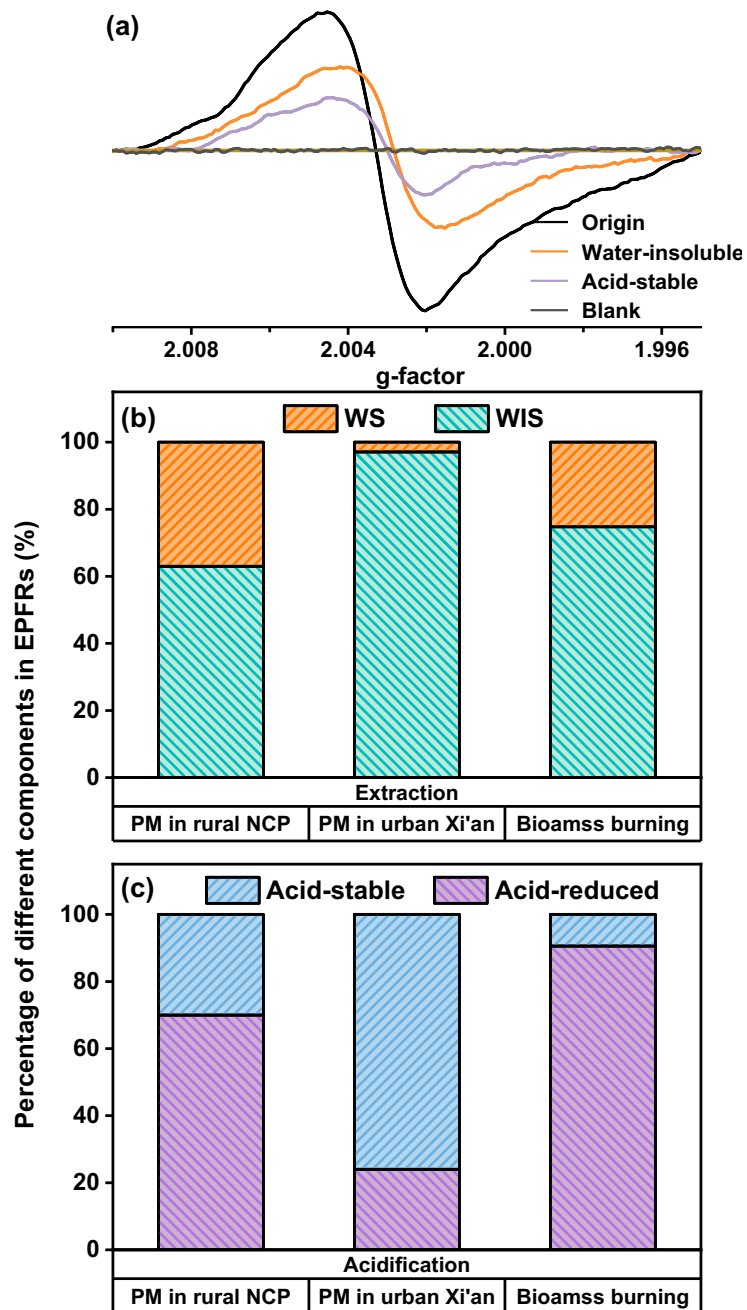
To demonstrate the possibly high solubility of EPFRs, additional experiments were conducted with PM filters extracted

by water prior to EPFRs analysis. On average, a 35.2% reduction in EPR signals was observed after water extraction (Figure 5), indicating that the same percentage of EPFRs was water-soluble (A detailed water-soluble fraction of EPFRs in each filter is listed in Table S8). This result is substantially higher than the reported water-soluble fraction (0.2%) of EPFRs in urban PM<sub>2.5</sub> of Xi'an (Figure 5b), where the majority of EPFRs likely consisted of graphene oxide analogues (Chen et al., 2018b). In addition, the result is also higher than that (11%) of EPFRs emitted from biomass burning (Guo et al., 2023), suggesting a high water-soluble fraction of EPFRs in the studied rural area.

It is widely acknowledged that EPFRs from combustion processes are formed through the electron transfer mediated by transition metals on organic combustion byproducts such as PAHs (Liu et al., 2022a; Vejerano et al., 2018). The EPR signal of these metal-EPFRs complexes can be substantially reduced (> 90%, Figure 5c) after acidification, as demonstrated by previous work (Guo et al., 2023). We also conducted the same acidification procedure and observed, on average, a 70% reduction in EPR signals (Figure 5c, detailed information is provided in Table S9). Although the reduction in our work is not as substantial as that of biomass-burning particles (Guo et al., 2023), the result indicates that there existed a large fraction of EPFRs in the form of metal-EPFRs complexes, likely originating from combustion sources (e.g., coal and biomass combustions). In addition, EPFRs showed significantly good correlations ( $r > 0.5$ ,  $p < 0.01$ ; Table S10) with certain transition metals species (i.e., Fe, Zn, Cr), suggesting their formation was likely associated with transition metals. The higher water-soluble fraction of EPFRs in our work compared to that of biomass-burning particles could be relevant to the increased polarity of EPFRs by atmospheric oxidation processes (i.e., the aging of metal-EPFRs complexes). It is also worth noting that the reduction of EPR signals is at a much greater extent than that (24%, Figure 5c) of EPFRs (mostly consisting of graphene oxide analogues) in urban PM<sub>2.5</sub> of Xi'an (Chen et al., 2018b).

In addition to the potentially oxidized/aged metal-EPFRs complexes, another significant source of water-soluble EPFRs could be EPFRs directly generated by secondary chemical processes. Chen et al. (2019) found that water-extracted humic-like

substances were the primary precursors of secondary EPFRs formed by visible-light illumination in ambient PM. A laboratory study by Tong et al. (2018) demonstrated that secondary organic aerosol formed by photooxidation of naphthalene contained EPFRs at levels comparable to those found in ambient PM. Given that atmospheric oxidation was the main source of EPFRs and PM in our studied region, these secondary chemical processes likely had a substantial impact on ambient PM, contributing to the formation of secondary EPFRs. However, further research is needed to fully elucidate and quantify the contribution of secondary formation pathways to water-soluble EPFRs.



335 **Figure 5.** (a) Gaussian fitting EPR spectra of a selected PM<sub>2.5</sub> filter sample (sampling date: 2023/03/12) before (black) and after water extraction (orange), as well as after acidification (green). A typical EPR spectrum of a blank filter (grey) is also present for reference. (b) The percentages of different fractionated EPFRs in rural NCP (this study), in urban PM of Xi'an (Chen et al., 2018b), and biomass burning particles (Guo et al., 2023).

Importantly, compared to total EPFRs, water-soluble EPFRs (WS-EPFRs) showed stronger correlations with WS-OP

340 (Figure 6) of  $PM_{2.5}$ . In addition, no significant correlation was observed between water-insoluble EPFRs (WIS-EPFRs) and WS-OP (Figures S11 a and b). These results demonstrate our hypothesis that the significant correlations between EPFRs and WS-OP were driven by the water-soluble fractions of EPFRs, while atmospheric oxidation processes had increased the water solubility of EPFRs. On the other hand, the lack of significant correlation between WIS-EPFRs and WIS-OP (Figures S11 c and d) could be attributed to the complex interplay of organics and metals affecting WIS-OP (Gao et al., 2020). Nonetheless, 345 the significant correlation between WS-EPFRs and WS-OP suggests that atmospheric oxidation processes may have contributed to the increased water solubility of EPFRs, thereby affecting their roles in  $PM_{2.5}$  oxidative potential.

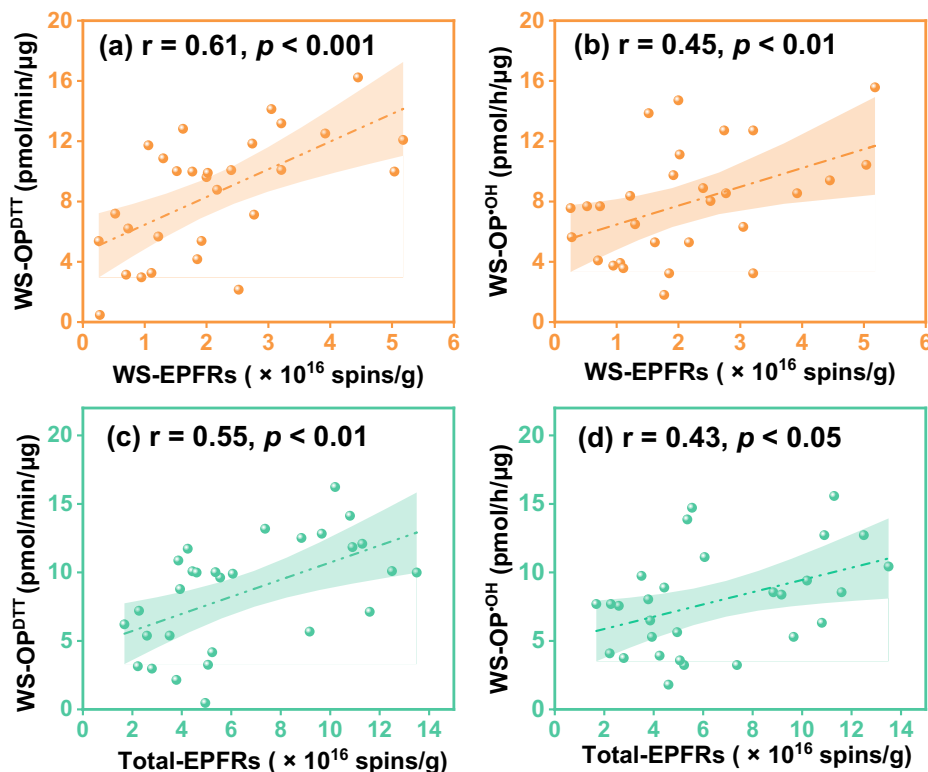


**Figure 6.** Correlation of WS/Total-EPFRs with WS-OP in  $PM_{2.5}$ ; (a) WS-EPFRs with  $WS-OP^{DTT}$  (b) WS-EPFRs with  $WS-OP^{OH}$ ; (c) Total-EPFRs with  $WS-OP^{DTT}$  (d) Total-EPFRs with  $WS-OP^{OH}$ . The Pearson correlation coefficients ( $r$ ) and associated  $p$  values are illustrated in the figure. The lines and shadow areas are linear regressions with their 95% confidence intervals.

#### 4. Conclusions and implications

In this study, EPFRs in fine, coarse, and total suspended particles in a typical rural region of the NCP have been investigated. The majority of EPFRs occurred in fine particles. EPFRs exhibited seasonal patterns distinct from those observed in urban environments. In addition, higher  $g$ -factors of EPFRs were identified compared to those reported for highway and urban PM, suggesting a greater extent of oxidation in rural EPFRs. These findings underscore a unique characteristic of EPFRs in rural areas, where local primary emissions of EPFRs are limited.

Additionally, atmospheric oxidation was resolved as the largest contributor to EPFRs. The atmospheric oxidation processes occurring during long-range/regional transport were suggested as the primary driver behind the more oxidized EPFRs observed in our work. We also demonstrated that the rural EPFRs contained a higher water-soluble fraction compared to those found in biomass burning particles and urban PM. Our results thus emphasize the importance of considering the water-soluble fraction of EPFRs, alongside their occurrence in organic solvent-extractable or non-extractable organics, particularly in regions without significant primary emissions of EPFRs. Future studies are warranted to investigate airborne EPFRs in other rural regions to yield a more complete understanding of the sources and properties of EPFRs, as only a typical rural site in NCP was examined in our work.

The WS-EPFRs could be an important contributor to the oxidative potential of  $PM_{2.5}$ , as suggested by their significant positive correlations. While prior research has predominantly focused on EPFRs in urban environments or originating from primary combustion emission sources, our findings revealed the evolution of EPFRs through atmospheric oxidation during transport (Figure 7). The atmospheric evolution of EPFRs may modify their properties, such as water solubility, thereby

altering their roles in contributing to the oxidative potential of PM (Wang et al., 2018c). It is also important to note that water-  
soluble EPFRs are more bioavailable than their insoluble forms. They are more likely to reach the tissues or organs beyond  
the lung deposition site, amplifying the threat to human health (Liu and Ng, 2023). Furthermore, beyond influencing the  
oxidative toxicity of PM, the role of evolved EPFRs in climate-related cloud chemistry may also change and should be explored  
in future research.

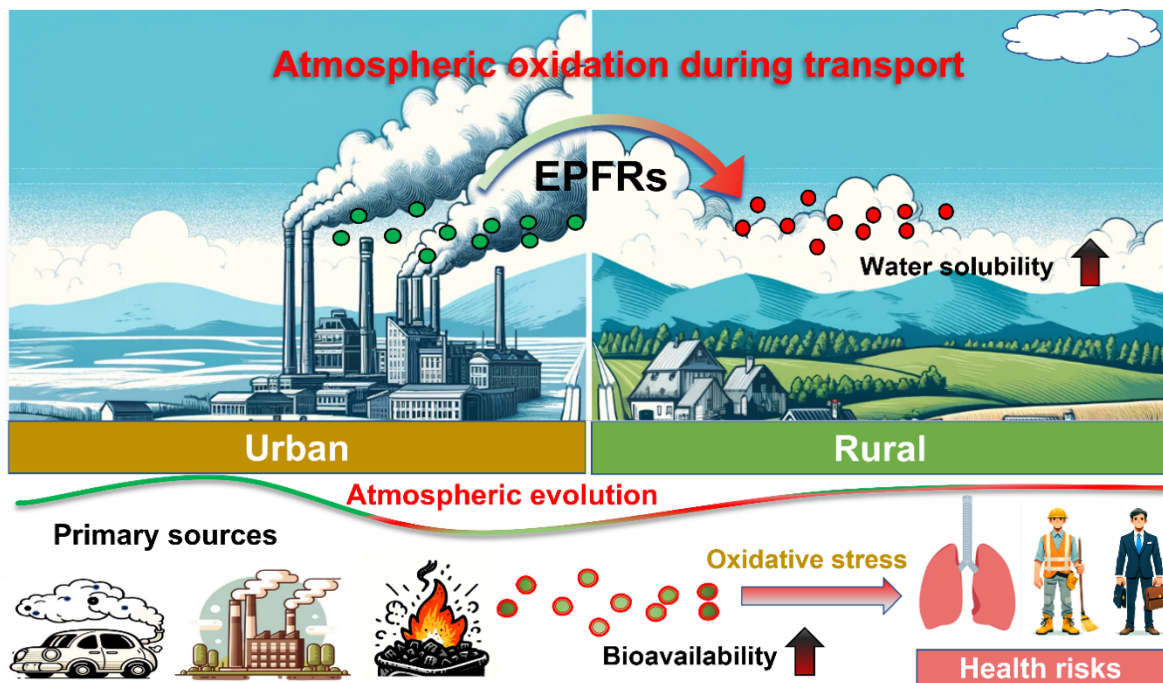


**Figure 7.** Implication of atmospheric evolution of EPFRs. EPFRs, primarily emitted from combustion sources, may undergo atmospheric oxidation during long-range/regional transport. This transformation may enhance the water solubility of EPFRs, potentially heightening their bioavailability and consequently elevating risks to human health.

Generally, soluble EPFRs are assumed to have a relatively short lifetime. For instance, it has been found that secondary EPFRs formed by photoexcitation are highly susceptible to reduction by oxygen, leading to short lifetimes ranging from  
approximately 30 minutes to one day (Chen et al., 2019). However, measurements conducted on several PM<sub>2.5</sub> filters stored at  
-20 °C for roughly one year showed that EPR signals only decreased by approximately 11% (Figure S12) suggesting the



persistency of EPFRs, including their water-soluble fraction. Previous research has indicated that semiquinone-type radicals adsorbed into a polymeric carbonaceous core (Valavanidis et al., 2005) or by electron transfer with transition metals (Truong et al., 2010) are stable and can have a lifetime longer than months. However, their water solubility remains unclear. Further efforts to identify the types of water-soluble EPFRs and investigate their lifetimes are warranted.

Overall, this study revealed the characteristics of EPFRs in rural regions, highlighting the importance of considering atmospheric oxidation processes in understanding their behavior and impacts. Future research efforts should aim to further elucidate the mechanisms governing the formation, evolution, and fate of EPFRs, as well as their interactions with other atmospheric components. Such insights are essential for developing effective strategies to mitigate the adverse effects of EPFRs on air quality and public health, as well as for advancing our understanding of their broader implications for atmospheric and environmental science.

#### **Data availability**

The data are available upon request to the corresponding author Fobang Liu ([fobang.liu@xjtu.edu.cn](mailto:fobang.liu@xjtu.edu.cn)) and Haijie Tong ([hajjie.tong@hereon.de](mailto:hajjie.tong@hereon.de)).

#### **Author contributions**

FL and XY designed the research. XY, SY, YY, YW, JL, MZ, and ZW carried out the experiments. FL, CH, HT, and KW supervised the study. FL and XY prepared the original manuscript with input from all the co-authors.

#### **Competing interests**

The authors declare that they have no conflict of interest.

## 400 **Disclaimer**

Publisher's note: Copernicus Publications remains neutral with regard to jurisdictional claims made in the text, published maps, institutional affiliations, or any other geographical representation in this paper. While Copernicus Publications makes every effort to include appropriate place names, the final responsibility lies with the authors. Regarding the maps used in this paper, please note that Figure S1 contains disputed territories.

## 405 **Acknowledgments**

This work is supported by the Natural Science Basic Research Program of Shaanxi (2023-JC-QN-0141), Qinchuanyuan introducing high-level innovation and entrepreneurship talent program (QCYRCXM-2022-363), and “Young Talent Support Plan” of Xi'an Jiaotong University (ND6J027). We gratefully acknowledge technical support from Professor Station of China Agricultural University at Xinzhou Center for Disease Control and Prevention. We acknowledge the use of ChatGPT 4.0 to  
410 generate the cartoons of Figure 7.

## **References**

Abrams, J. Y., Weber, R. J., Klein, M., Sarnat, S. E., Chang, H. H., Strickland, M. J., Verma, V., Fang, T., Bates, J. T., Mulholland, J. A., Russell, A. G., and Tolbert, P. E.: Associations between Ambient Fine Particulate Oxidative Potential and Cardiorespiratory Emergency Department Visits, *Environ. Health Perspect.*, 125, 9, <https://doi.org/10.1289/ehp3048>, 2017.

415 Ai, J., Qin, W. H., Chen, J., Sun, Y. W., Yu, Q., Xin, K., Huang, H. Y., Zhang, L. Y., Ahmad, M., and Liu, X. A.: Pollution characteristics and light-driven evolution of environmentally persistent free radicals in PM<sub>2.5</sub> in two typical northern cities of China, *J. Hazard. Mater.*, 454, 131466, <https://doi.org/10.1016/j.jhazmat.2023.131466>, 2023.

Ainur, D., Chen, Q. C., Wang, Y. Q., Li, H., Lin, H., Ma, X. Y., and Xu, X.: Pollution characteristics and sources of environmentally persistent free radicals and oxidation potential in fine particulate matter related to city lockdown (CLD) in  
420 Xi'an, China, *Environ. Res.*, 210, 11, <https://doi.org/10.1016/j.envres.2022.112899>, 2022.

- Ainur, D., Chen, Q. C., Sha, T., Zarak, M., Dong, Z. P., Guo, W., Zhang, Z. M., Dina, K., and An, T. C.: Outdoor Health Risk of Atmospheric Particulate Matter at Night in Xi'an, Northwestern China, *Environ. Sci. Technol.*, 57, 9252-9265, <https://doi.org/10.1021/acs.est.3c02670>, 2023.
- Alleman, L. Y., Lamaison, L., Perdrix, E., Robache, A., and Galloo, J. C.: PM<sub>10</sub> metal concentrations and source identification using positive matrix factorization and wind sectoring in a French industrial zone, *Atmos. Res.*, 96, 612-625, <https://doi.org/10.1016/j.atmosres.2010.02.008>, 2010.
- 425 An, J. L., Duan, Q., Wang, H. L., Miao, Q., Shao, P., Wang, J., and Zou, J. N.: Fine particulate pollution in the Nanjing northern suburb during summer: composition and sources, *Environ. Monit. Assess.*, 187, 561, <https://doi.org/10.1007/s10661-015-4765-2>, 2015.
- 430 Arangio, A. M., Tong, H. J., Socorro, J., Pöschl, U., and Shiraiwa, M.: Quantification of environmentally persistent free radicals and reactive oxygen species in atmospheric aerosol particles, *Atmos. Chem. Phys.*, 16, 13105-13119, <https://doi.org/10.5194/acp-16-13105-2016>, 2016.
- Balakrishna, S., Lomnicki, S., McAvey, K. M., Cole, R. B., Dellinger, B., and Cormier, S. A.: Environmentally persistent free radicals amplify ultrafine particle mediated cellular oxidative stress and cytotoxicity, *Part. Fibre Toxicol.*, 6, 11, <https://doi.org/10.1186/1743-8977-6-11>, 2009.
- 435 Begum, B. A., Biswas, S. K., and Hopke, P. K.: Key issues in controlling air pollutants in Dhaka, Bangladesh, *Atmos. Environ.*, 45, 7705-7713, <https://doi.org/10.1016/j.atmosenv.2010.10.022>, 2011.
- Bhattu, D., Tripathi, S. N., Bhowmik, H. S., Moschos, V., Lee, C. P., Rauber, M., Salazar, G., Abbaszade, G., Cui, T., Slowik, J. G., Vats, P., Mishra, S., Lalchandani, V., Satish, R., Rai, P., Casotto, R., Tobler, A., Kumar, V., Hao, Y., and Qi, L.: Local incomplete combustion emissions define the PM<sub>2.5</sub> oxidative potential in Northern India, *Nat. Commun.*, 15, 3517, <https://doi.org/10.1038/s41467-024-47785-5>, 2024.
- 440 Borrowman, C. K., Zhou, S. M., Burrow, T. E., and Abbatt, J. P. D.: Formation of environmentally persistent free radicals from the heterogeneous reaction of ozone and polycyclic aromatic compounds, *Phys. Chem. Chem. Phys.*, 18, 205-212, <https://doi.org/10.1039/c5cp05606c>, 2016.
- 445 Brown, S. G., Eberly, S., Paatero, P., and Norris, G. A.: Methods for estimating uncertainty in PMF solutions: Examples with ambient air and water quality data and guidance on reporting PMF results, *Sci. Total Environ.*, 518, 626-635, <https://doi.org/10.1016/j.scitotenv.2015.01.022>, 2015.
- Calas, A., Uzu, G., Kelly, F. J., Houdier, S., Martins, J. M. F., Thomas, F., Molton, F., Charron, A., Dunster, C., Oliete, A., Jacob, V., Besombes, J. L., Chevrier, F., and Jaffrezo, J. L.: Comparison between five acellular oxidative potential measurement assays performed with detailed chemistry on PM<sub>10</sub> samples from the city of Chamonix (France), *Atmos. Chem. Phys.*, 18, 7863-7875, <https://doi.org/10.5194/acp-18-7863-2018>, 2018.
- 450

- Campbell, S. J., Wolfer, K., Utinger, B., Westwood, J., Zhang, Z. H., Bukowiecki, N., Steimer, S. S., Vu, T. V., Xu, J. S., Straw, N., Thomson, S., Elzein, A., Sun, Y. L., Liu, D., Li, L. J., Fu, P. Q., Lewis, A. C., Harrison, R. M., Bloss, W. J., Loh, M., Miller, M. R., Shi, Z. B., and Kalberer, M.: Atmospheric conditions and composition that influence PM<sub>2.5</sub> oxidative potential in Beijing, China, *Atmos. Chem. Phys.*, 21, 5549-5573, <https://doi.org/10.5194/acp-21-5549-2021>, 2021.
- 455 Cao, J. J., Wu, F., Chow, J. C., Lee, S. C., Li, Y., Chen, S. W., An, Z. S., Fung, K. K., Watson, J. G., Zhu, C. S., and Liu, S. X.: Characterization and source apportionment of atmospheric organic and elemental carbon during fall and winter of 2003 in Xi'an, China, *Atmos. Chem. Phys.*, 5, 3127-3137, <https://doi.org/10.5194/acp-5-3127-2005>, 2005.
- Charrier, J. G. and Anastasio, C.: Rates of Hydroxyl Radical Production from Transition Metals and Quinones in a Surrogate Lung Fluid, *Environ. Sci. Technol.*, 49, 9317-9325, <https://doi.org/10.1021/acs.est.5b01606>, 2015.
- 460 Chen, Q. C., Sun, H. Y., Song, W. H., Cao, F., Tian, C. G., and Zhang, Y. L.: Size-resolved exposure risk of persistent free radicals (EPFRs) in atmospheric aerosols and their potential sources, *Atmos. Chem. Phys.*, 20, 14407-14417, <https://doi.org/10.5194/acp-20-14407-2020>, 2020.
- Chen, Q. C., Sun, H. Y., Wang, M. M., Wang, Y. Q., Zhang, L. X., and Han, Y. M.: Environmentally Persistent Free Radical (EPFR) Formation by Visible-Light Illumination of the Organic Matter in Atmospheric Particles, *Environ. Sci. Technol.*, 53, 10053-10061, <https://doi.org/10.1021/acs.est.9b02327>, 2019.
- 465 Chen, Q. C., Wang, M. M., Sun, H. Y., Wang, X., Wang, Y. Q., Li, Y. G., Zhang, L. X., and Mu, Z.: Enhanced health risks from exposure to environmentally persistent free radicals and the oxidative stress of PM<sub>2.5</sub> from Asian dust storms in Erenhot, Zhangbei and Jinan, China, *Environ. Int.*, 121, 260-268, <https://doi.org/10.1016/j.envint.2018.09.012>, 2018a.
- 470 Chen, Q. C., Sun, H. Y., Wang, M. M., Mu, Z., Wang, Y. Q., Li, Y. G., Wang, Y. S., Zhang, L. X., and Zhang, Z. M.: Dominant Fraction of EPFRs from Nonsolvent-Extractable Organic Matter in Fine Particulates over Xi'an, China, *Environ. Sci. Technol.*, 52, 9646-9655, <https://doi.org/10.1021/acs.est.8b01980>, 2018b.
- Comandini, A., Malewicki, T., and Brezinsky, K.: Chemistry of Polycyclic Aromatic Hydrocarbons Formation from Phenyl Radical Pyrolysis and Reaction of Phenyl and Acetylene, *J. Phys. Chem. A.*, 116, 2409-2434, <https://doi.org/10.1021/jp207461a>, 2012.
- 475 Cormier, S. A., Lomnicki, S., Backes, W., and Dellinger, B.: Origin and health impacts of emissions of toxic by-products and fine particles from combustion and thermal treatment of hazardous wastes and materials, *Environ. Health Perspect.*, 114, 810-817, <https://doi.org/10.1289/ehp.8629>, 2006.
- Daellenbach, K. R., Uzu, G., Jiang, J. H., Cassagnes, L. E., Leni, Z., Vlachou, A., Stefanelli, G., Canonaco, F., Weber, S., Segers, A., Kuenen, J. J. P., Schaap, M., Favez, O., Albinet, A., Aksoyoglu, S., Dommen, J., Baltensperger, U., Geiser, M., El Haddad, I., Jaffrezo, J. L., and Prévôt, A. S. H.: Sources of particulate-matter air pollution and its oxidative potential in Europe, *Nature.*, 587, 414-419, <https://doi.org/10.1038/s41586-020-2902-8>, 2020.

- 485 Dalal, N. S., Jafari, B., Petersen, M., Green, F. H. Y., and Vallyathan, V.: Presence of stable coal radicals in autopsied coal miners' lungs and its possible correlation to coal workers' pneumoconiosis, *Arch. Environ. Health.*, 46, 366-372, <https://doi.org/10.1080/00039896.1991.9934404>, 1991.
- Dong, Z., Wang, S. B., Sun, J. B., Shang, L. Q., Li, Z. H., and Zhang, R. Q.: Impact of COVID-19 lockdown on carbonaceous aerosols in a polluted city: Composition characterization, source apportionment, influence factors of secondary formation, *Chemosphere.*, 307, 11, <https://doi.org/10.1016/j.chemosphere.2022.136028>, 2022.
- 490 Dugas, T. R., Lomnicki, S., Cormier, S. A., Dellinger, B., and Reams, M.: Addressing Emerging Risks: Scientific and Regulatory Challenges Associated with Environmentally Persistent Free Radicals, *Int. J. Environ. Res. Public Health.*, 13, 17, <https://doi.org/10.3390/ijerph13060573>, 2016.
- Fang, T., Lakey, P. S. J., Weber, R. J., and Shiraiwa, M.: Oxidative Potential of Particulate Matter and Generation of Reactive Oxygen Species in Epithelial Lining Fluid, *Environ. Sci. Technol.*, 53, 12784-12792, <https://doi.org/10.1021/acs.est.9b03823>, 2019.
- 495 Fang, T., Verma, V., Guo, H., King, L. E., and Edgerton, E. S.: A semi-automated system for quantifying the oxidative potential of ambient particles in aqueous extracts using the dithiothreitol (DTT) assay: results from the Southeastern Center for Air Pollution and Epidemiology (SCAPE), *Atmos. Meas. Tech.*, 8, 471-482, <https://doi.org/10.5194/amt-8-471-2015>, 2015.
- Fang, T., Hwang, B. C. H., Kapur, S., Hopstock, K. S., Wei, J. L., Nguyen, V., Nizkorodov, S. A., and Shiraiwa, M.: Wildfire particulate matter as a source of environmentally persistent free radicals and reactive oxygen species, *Environ. Sci.-Atmospheres.*, 3, 581-594, <https://doi.org/10.1039/d2ea00170e>, 2023.
- 500 Filippi, A., Sheu, R., Berkemeier, T., Pöschl, U., Tong, H., and Gentner, D. R.: Environmentally persistent free radicals in indoor particulate matter, dust, and on surfaces, *Environ. Sci.-Atmospheres.*, 2, 128-136, <https://doi.org/10.1039/d1ea00075f>, 2022.
- Gao, D., Mulholland, J. A., Russell, A. G., and Weber, R. J.: Characterization of the water-insoluble oxidative potential of PM<sub>2.5</sub> using the dithiothreitol assay, *Atmos. Environ.*, 224, 117327, <https://doi.org/10.1016/j.atmosenv.2020.117327>, 2020.
- 505 Gao, D., Fang, T., Verma, V., Zeng, L. G., and Weber, R. J.: A method for measuring total aerosol oxidative potential (OP) with the dithiothreitol (DTT) assay and comparisons between an urban and roadside site of water-soluble and total OP, *Atmos. Meas. Tech.*, 10, 2821-2835, <https://doi.org/10.5194/amt-10-2821-2017>, 2017.
- Gao, J., Huang, J., Li, X., Tian, G., Wang, X., Yang, C., and Ma, C.: Challenges of the UK government and industries regarding emission control after ICE vehicle bans, *Sci. Total Environ.*, 835, 155406, <https://doi.org/10.1016/j.scitotenv.2022.155406>, 2022.
- 510 Gehling, W. and Dellinger, B.: Environmentally Persistent Free Radicals and Their Lifetimes in PM<sub>2.5</sub>, *Environ. Sci. Technol.*, 47, 8172-8178, <https://doi.org/10.1021/es401767m>, 2013.

- 515 Gehling, W., Khachatryan, L., and Dellinger, B.: Hydroxyl Radical Generation from Environmentally Persistent Free Radicals (EPFRs) in PM<sub>2.5</sub>, *Environ. Sci. Technol.*, 48, 4266-4272, <https://doi.org/10.1021/es401770y>, 2014.
- Guo, H. B., Wang, Y. D., Yao, K. X., Zheng, H., Zhang, X. J., Li, R., Wang, N., and Fu, H. Y.: The overlooked formation of environmentally persistent free radicals on particulate matter collected from biomass burning under light irradiation, *Environ. Int.*, 171, 10, <https://doi.org/10.1016/j.envint.2022.107668>, 2023.
- 520 Guo, X. W., Zhang, N., Hu, X., Huang, Y., Ding, Z. H., Chen, Y. J., and Lian, H. Z.: Characteristics and potential inhalation exposure risks of PM<sub>2.5</sub>-bound environmental persistent free radicals in Nanjing, a mega-city in China, *Atmos. Environ.*, 224, 117355, <https://doi.org/10.1016/j.atmosenv.2020.117355>, 2020.
- Heo, J. B., Dulger, M., Olson, M. R., McGinnis, J. E., Shelton, B. R., Matsunaga, A., Sioutas, C., and Schauer, J. J.: Source apportionments of PM<sub>2.5</sub> organic carbon using molecular marker Positive Matrix Factorization and comparison of results from different receptor models, *Atmos. Environ.*, 73, 51-61, <https://doi.org/10.1016/j.atmosenv.2013.03.004>, 2013.
- 525 Hwang, B., Fang, T., Pham, R., Wei, J. L., Gronstal, S., Lopez, B., Frederickson, C., Galeazzo, T., Wang, X. L., Jung, H., and Shiraiwa, M.: Environmentally Persistent Free Radicals, Reactive Oxygen Species Generation, and Oxidative Potential of Highway PM<sub>2.5</sub>, *ACS Earth Space Chem.*, 5, 1865-1875, <https://doi.org/10.1021/acsearthspacechem.1c00135>, 2021.
- Ikemori, F., Uranishi, K., Asakawa, D., Nakatsubo, R., Makino, M., Kido, M., Mitamura, N., Asano, K., Nonaka, S., Nishimura, R., and Sugata, S.: Source apportionment in PM<sub>2.5</sub> in central Japan using positive matrix factorization focusing on small-scale
- 530 local biomass burning, *Atmos. Pollut. Res.*, 12, 349-359, <https://doi.org/10.1016/j.apr.2021.01.006>, 2021.
- Jang, E., Jeong, T., Yoon, N., and Jeong, S.: Source apportionment of airborne PCDD/F at industrial and urban sites in Busan, South Korea, *Chemosphere.*, 239, 124717, <https://doi.org/10.1016/j.chemosphere.2019.124717>, 2020.
- Jia, H. Z., Zhao, S., Nulaji, G., Tao, K. L., Wang, F., Sharma, V. K., and Wang, C. Y.: Environmentally Persistent Free Radicals in Soils of Past Coking Sites: Distribution and Stabilization, *Environ. Sci. Technol.*, 51, 6000-6008, <https://doi.org/10.1021/acs.est.7b00599>, 2017.
- 535 Jia, S.-M., Wang, D.-Q., Liu, L.-Y., Zhang, Z.-F., and Ma, W.-L.: Size-resolved environmentally persistent free radicals in cold region atmosphere: Implications for inhalation exposure risk, *J. Hazard. Mater.*, 443, 130263, <https://doi.org/10.1016/j.jhazmat.2022.130263>, 2023.
- Jin, L., Xie, J. W., Wong, C. K. C., Chan, S. K. Y., Abbaszade, G., Schnelle-Kreis, J., Zimmermann, R., Li, J., Zhang, G., Fu, P. Q., and Li, X. D.: Contributions of City-Specific Fine Particulate Matter (PM<sub>2.5</sub>) to Differential in Vitro Oxidative Stress and Toxicity Implications between Beijing and Guangzhou of China, *Environ. Sci. Technol.*, 53, 2881-2891, <https://doi.org/10.1021/acs.est.9b00449>, 2019.
- 540 Johnson, K. S., de Foy, B., Zuberi, B., Molina, L. T., Molina, M. J., Xie, Y., Laskin, A., and Shutthanandan, V.: Aerosol composition and source apportionment in the Mexico City Metropolitan Area with PIXE/PESA/STIM and multivariate analysis, *Atmos. Chem. Phys.*, 6, 4591-4600, <https://doi.org/10.5194/acp-6-4591-2006>, 2006.
- 545

- Khobragade, P. P. and Ahirwar, A. V.: Source identification and ambient trace element concentrations of PM<sub>10</sub> using receptor modeling in an urban area of Chhattisgarh, India, *Geocarto Int.*, 37, 12267-12293, <https://doi.org/10.1080/10106049.2022.2066201>, 2022.
- Kim, E. and Hopke, P. K.: Improving source identification of fine particles in a rural northeastern US area utilizing temperature-resolved carbon fractions, *Journal of Geophysical Research-Atmospheres.*, 109, 13, <https://doi.org/10.1029/2003jd004199>, 2004.
- Kundu, S., Kawamura, K., Andreae, T. W., Hoffer, A., and Andreae, M. O.: Diurnal variation in the water-soluble inorganic ions, organic carbon and isotopic compositions of total carbon and nitrogen in biomass burning aerosols from the LBA-SMOCC campaign in Rondonia, Brazil, *J. Aerosol Sci.*, 41, 118-133, <https://doi.org/10.1016/j.jaerosci.2009.08.006>, 2010.
- 555 Lei, M., Huang, X. Z., Wang, C. B., Yan, W. Q., and Wang, S. L.: Investigation on SO<sub>2</sub>, NO and NO<sub>2</sub> release characteristics of Datong bituminous coal during pressurized oxy-fuel combustion, *J. Therm. Anal. Calorim.*, 126, 1067-1075, <https://doi.org/10.1007/s10973-016-5652-y>, 2016.
- Li, C., Hakkim, H., Sinha, V., Sinha, B., Pardo, M., Cai, D., Reicher, N., Chen, J., Hao, K., and Rudich, Y.: Variation of PM<sub>2.5</sub> Redox Potential and Toxicity During Monsoon in Delhi, India, *ACS ES&T Air.*, 1, 316-329, <https://doi.org/10.1021/acsestair.3c00096>, 2024.
- 560 Li, H., Chen, Q. C., Wang, C., Wang, R. H., Sha, T., Yang, X. Q., and Ainur, D.: Pollution characteristics of environmental persistent free radicals (EPFRs) and their contribution to oxidation potential in road dust in a large city in northwest China, *J. Hazard. Mater.*, 442, 130087, <https://doi.org/10.1016/j.jhazmat.2022.130087>, 2023.
- Li, X. Y., Kuang, X. B. M., Yan, C. Q., Ma, S. X., Paulson, S. E., Zhu, T., Zhang, Y. H., and Zheng, M.: Oxidative Potential by PM<sub>2.5</sub> in the North China Plain: Generation of Hydroxyl Radical, *Environ. Sci. Technol.*, 53, 512-520, <https://doi.org/10.1021/acs.est.8b05253>, 2019.
- 565 Liu, F. and Ng, N. L.: *Toxicity of Atmospheric Aerosols: Methodologies & Assays*, American Chemical Society, Washington, DC, <https://doi.org/10.1021/acsinfocus.7e7012>, 2023.
- Liu, S. J., Huang, W. L., Yang, J. J., Xiong, Y., Huang, Z. Q., Wang, J. L., Cai, T. T., Dang, Z., and Yang, C.: Formation of environmentally persistent free radicals on microplastics under UV irradiations, *J. Hazard. Mater.*, 453, 10, <https://doi.org/10.1016/j.jhazmat.2023.131277>, 2023.
- 570 Liu, S. T., Liu, G. R., Yang, L. L., Liu, X. Y., Wang, M. X., Qin, L. J., and Zheng, M. H.: Metal-Catalyzed Formation of Organic Pollutants Intermediated by Organic Free Radicals, *Environ. Sci. Technol.*, 56, 14550-14561, <https://doi.org/10.1021/acs.est.2c05892>, 2022a.
- 575 Liu, X. Y., Yang, L. L., Liu, G. R., and Zheng, M. H.: Formation of Environmentally Persistent Free Radicals during Thermochemical Processes and their Correlations with Unintentional Persistent Organic Pollutants, *Environ. Sci. Technol.*, 55, 6529-6541, <https://doi.org/10.1021/acs.est.0c08762>, 2021.

- Liu, Y., Wang, R. S., Zhao, T. N., Zhang, Y., Wang, J. H., Wu, H. X., and Hu, P.: Source apportionment and health risk due to PM<sub>10</sub> and TSP at the surface workings of an underground coal mine in the arid desert region of northwestern China, *Sci. Total Environ.*, 803, 149901, <https://doi.org/10.1016/j.scitotenv.2021.149901>, 2022b.
- 580 Nagpure, A. S., Gurjar, B. R., Kumar, V., and Kumar, P.: Estimation of exhaust and non-exhaust gaseous, particulate matter and air toxics emissions from on-road vehicles in Delhi, *Atmos. Environ.*, 127, 118-124, <https://doi.org/10.1016/j.atmosenv.2015.12.026>, 2016.
- Ni, Z., Gao, N., Chen, N., Zhang, C., Liu, Z., Zhu, K. C., Sharma, V. K., and Jia, H. Z.: Particle-size distributions of environmentally persistent free radicals and oxidative potential of soils from a former gasworks site, *Sci. Total Environ.*, 869, 9, <https://doi.org/10.1016/j.scitotenv.2023.161747>, 2023.
- 585 Pryor, W. A., Prier, D. G., and Church, D. F.: Electron-spin resonance study of mainstream and sidestream cigarette smoke: nature of the free radicals in gasphase smoke and in cigarette tar, *Environ. Health Perspect.*, 47, 345-355, <https://doi.org/10.1289/ehp.8347345>, 1983.
- 590 Qin, L. J., Yang, L. L., Yang, J. H., Weber, R., Rangelova, K., Liu, X. Y., Lin, B. C., Li, C., Zheng, M. H., and Liu, G. R.: Photoinduced formation of persistent free radicals, hydrogen radicals, and hydroxyl radicals from catechol on atmospheric particulate matter, *iscience.*, 24, 102193, <https://doi.org/10.1016/j.isci.2021.102193>, 2021.
- Ramadan, Z., Song, X. H., and Hopke, P. K.: Identification of sources of Phoenix aerosol by positive matrix factorization, *J. Air Waste Manage. Assoc.*, 50, 1308-1320, <https://doi.org/10.1080/10473289.2000.10464173>, 2000.
- 595 Ramya, C. B., Aswini, A. R., Hegde, P., Boreddy, S. K. R., and Babu, S. S.: Water-soluble organic aerosols over South Asia- Seasonal changes and source characteristics, *Sci. Total Environ.*, 900, 10, <https://doi.org/10.1016/j.scitotenv.2023.165644>, 2023.
- Reff, A., Eberly, S. I., and Bhawe, P. V.: Receptor modeling of ambient particulate matter data using positive matrix factorization: Review of existing methods, *J. Air Waste Manage. Assoc.*, 57, 146-154, <https://doi.org/10.1080/10473289.2007.10465319>, 600 2007.
- Runberg, H. L., Mitchell, D. G., Eaton, S. S., Eaton, G. R., and Majestic, B. J.: Stability of environmentally persistent free radicals (EPFR) in atmospheric particulate matter and combustion particles, *Atmos. Environ.*, 240, 117809, <https://doi.org/10.1016/j.atmosenv.2020.117809>, 2020.
- Sarmiento, D. J. and Majestic, B. J.: Formation of Environmentally Persistent Free Radicals from the Irradiation of Polycyclic Aromatic Hydrocarbons, *J. Phys. Chem. A.*, 127, 5390-5401, <https://doi.org/10.1021/acs.jpca.3c01405>, 2023.
- 605 Sharma, S. K., Mandal, T. K., Saxena, M., Sharma, R. A., Datta, A., and Saud, T.: Variation of OC, EC, WSIC and trace metals of PM<sub>10</sub> in Delhi, India, *J. Atmos. Sol. Terr. Phys.*, 113, 10-22, <https://doi.org/10.1016/j.jastp.2014.02.008>, 2014.



- Shiraiwa, M., Sosedova, Y., Rouvière, A., Yang, H., Zhang, Y. Y., Abbatt, J. P. D., Ammann, M., and Pöschl, U.: The role of long-lived reactive oxygen intermediates in the reaction of ozone with aerosol particles, *Nat. Chem.*, 3, 291-295, <https://doi.org/10.1038/nchem.988>, 2011.
- 610
- Son, Y., Mishin, V., Welsh, W., Lu, S. E., Laskin, J. D., Kipen, H., and Meng, Q. M.: A Novel High-Throughput Approach to Measure Hydroxyl Radicals Induced by Airborne Particulate Matter, *Int. J. Environ. Res. Public Health.*, 12, 13678-13695, <https://doi.org/10.3390/ijerph121113678>, 2015.
- Stanimirova, I., Rich, D. Q., Russell, A. G., and Hopke, P. K.: A long-term, dispersion normalized PMF source apportionment of PM<sub>2.5</sub> in Atlanta from 2005 to 2019, *Atmos. Environ.*, 312, 10, <https://doi.org/10.1016/j.atmosenv.2023.120027>, 2023.
- 615
- Tian, L. W., Koshland, C. P., Yano, J. K., Yachandra, V. K., Yu, I. T. S., Lee, S. C., and Lucas, D.: Carbon-Centered Free Radicals in Particulate Matter Emissions from Wood and Coal Combustion, *Energy & Fuels.*, 23, 2523-2526, <https://doi.org/10.1021/ef8010096>, 2009.
- Tong, H. J., Lakey, P. S. J., Arangio, A. M., Socorro, J., Shen, F. X., Lucas, K., Brune, W. H., Pöschl, U., and Shiraiwa, M.: Reactive Oxygen Species Formed by Secondary Organic Aerosols in Water and Surrogate Lung Fluid, *Environ. Sci. Technol.*, 52, 11642-11651, <https://doi.org/10.1021/acs.est.8b03695>, 2018.
- 620
- Truong, H., Lomnicki, S., and Dellinger, B.: Potential for Misidentification of Environmentally Persistent Free Radicals as Molecular Pollutants in Particulate Matter, *Environ. Sci. Technol.*, 44, 1933-1939, <https://doi.org/10.1021/es902648t>, 2010.
- Valavanidis, A., Fiotakis, K., Bakeas, E., and Vlahogianni, T.: Electron paramagnetic resonance study of the generation of reactive oxygen species catalysed by transition metals and quinoid redox cycling by inhalable ambient particulate matter, *Redox Rep.*, 10, 37-51, <https://doi.org/10.1179/135100005X21606>, 2005.
- 625
- Vejerano, E. P. and Ahn, J.: Leaves are a Source of Biogenic Persistent Free Radicals, *Environ. Sci. Technol. Lett.*, 10, 662-667, <https://doi.org/10.1021/acs.estlett.3c00277>, 2023.
- Vejerano, E. P., Rao, G. Y., Khachatryan, L., Cormier, S. A., and Lomnicki, S.: Environmentally Persistent Free Radicals: Insights on a New Class of Pollutants, *Environ. Sci. Technol.*, 52, 2468-2481, <https://doi.org/10.1021/acs.est.7b04439>, 2018.
- 630
- Verma, V., Rico-Martinez, R., Kotra, N., King, L., Liu, J. M., Snell, T. W., and Weber, R. J.: Contribution of Water-Soluble and Insoluble Components and Their Hydrophobic/Hydrophilic Subfractions to the Reactive Oxygen Species-Generating Potential of Fine Ambient Aerosols, *Environ. Sci. Technol.*, 46, 11384-11392, <https://doi.org/10.1021/es302484r>, 2012.
- Wang, C., Huang, Y. P., Zhang, Z. T., and Cai, Z. W.: Levels, spatial distribution, and source identification of airborne environmentally persistent free radicals from tree leaves, *Environ. Pollut.*, 257, 11353, <https://doi.org/10.1016/j.envpol.2019.113353>, 2020a.
- 635
- Wang, C. A., Wang, P. Q., Zhao, L., Du, Y. B., and Che, D. F.: Experimental Study on NO<sub>x</sub> Reduction in Oxy-fuel Combustion Using Synthetic Coals with Pyridinic or Pyrrolic Nitrogen, *Appl. Sci.-Basel.*, 8, 12, <https://doi.org/10.3390/app8122499>, 2018a.

- 640 Wang, P., Pan, B., Li, H., Huang, Y., Dong, X. D., Ai, F., Liu, L. Y., Wu, M., and Xing, B. S.: The Overlooked Occurrence of Environmentally Persistent Free Radicals in an Area with Low-Rank Coal Burning, Xuanwei, China, *Environ. Sci. Technol.*, 52, 1054-1061, <https://doi.org/10.1021/acs.est.7b05453>, 2018b.
- Wang, P. L., Thevenot, P., Saravia, J., Ahlert, T., and Cormier, S. A.: Radical-Containing Particles Activate Dendritic Cells and Enhance Th17 Inflammation in a Mouse Model of Asthma, *Am. J. Respir. Cell Mol. Biol.*, 45, 977-983, <https://doi.org/10.1165/rcmb.2011-0001OC>, 2011.
- 645 Wang, S. Y., Ye, J. H., Soong, R., Wu, B., Yu, L. G., Simpson, A. J., and Chan, A. W. H.: Relationship between chemical composition and oxidative potential of secondary organic aerosol from polycyclic aromatic hydrocarbons, *Atmos. Chem. Phys.*, 18, 3987-4003, <https://doi.org/10.5194/acp-18-3987-2018>, 2018c.
- Wang, Y. D., Yao, K. X., Fu, X., Zhai, X. Y., Jin, L., and Guo, H. B.: Size-resolved exposure risk and subsequent role of environmentally persistent free radicals (EPFRs) from atmospheric particles, *Atmos. Environ.*, 276, 9, <https://doi.org/10.1016/j.atmosenv.2022.119059>, 2022.
- 650 Wang, Y. Q., Li, S. P., Wang, M. M., Sun, H. Y., Mu, Z., Zhang, L. X., Li, Y. G., and Chen, Q. C.: Source apportionment of environmentally persistent free radicals (EPFRs) in PM<sub>2.5</sub> over Xi'an, China, *Sci. Total Environ.*, 689, 193-202, <https://doi.org/10.1016/j.scitotenv.2019.06.424>, 2019.
- Wang, Y. Q., Wang, M. M., Li, S. P., Sun, H. Y., Mu, Z., Zhang, L. X., Li, Y. G., and Chen, Q. C.: Study on the oxidation potential of the water-soluble components of ambient PM<sub>2.5</sub> over Xi'an, China: Pollution levels, source apportionment and transport pathways, *Environ. Int.*, 136, 11, <https://doi.org/10.1016/j.envint.2020.105515>, 2020b.
- 655 Weichenthal, S., Lavigne, E., Evans, G., Pollitt, K., and Burnett, R. T.: Ambient PM<sub>2.5</sub> and risk of emergency room visits for myocardial infarction: impact of regional PM<sub>2.5</sub> oxidative potential: a case-crossover study, *Environ. Health.*, 15, 9, <https://doi.org/10.1186/s12940-016-0129-9>, 2016.
- 660 Xu, Y., Yang, L. L., Wang, X. P., Zheng, M. H., Li, C., Zhang, A. Q., Fu, J. J., Yang, Y. P., Qin, L. J., Liu, X. Y., and Liu, G. R.: Risk evaluation of environmentally persistent free radicals in airborne particulate matter and influence of atmospheric factors, *Ecotoxicol. Environ. Saf.*, 196, 9, <https://doi.org/10.1016/j.ecoenv.2020.110571>, 2020.
- Yang, L. L., Liu, G. R., Zheng, M. H., Jin, R., Zhu, Q. Q., Zhao, Y. Y., Wu, X. L., and Xu, Y.: Highly Elevated Levels and Particle-Size Distributions of Environmentally Persistent Free Radicals in Haze-Associated Atmosphere, *Environ. Sci. Technol.*, 51, 7936-7944, <https://doi.org/10.1021/acs.est.7b01929>, 2017.
- 665 Yang, Y., Battaglia, M. A., Mohan, M. K., Robinson, E. S., DeCarlo, P. F., Edwards, K. C., Fang, T., Kapur, S., Shiraiwa, M., Cesler-Maloney, M., Simpson, W. R., Campbell, J. R., Nenes, A., Mao, J., and Weber, R. J.: Assessing the Oxidative Potential of Outdoor PM<sub>2.5</sub> in Wintertime Fairbanks, Alaska, *ACS ES&T Air*, 1, 175-187, <https://doi.org/10.1021/acsestair.3c00066>, 2024.

- 670 Yi, J.-F., Lin, Z.-Z., Li, X., Zhou, Y.-Q., and Guo, Y.: A short review on environmental distribution and toxicity of the environmentally persistent free radicals, *Chemosphere.*, 340, 139922, <https://doi.org/10.1016/j.chemosphere.2023.139922>, 2023.
- Yu, H. R., Wei, J. L., Cheng, Y. L., Subedi, K., and Verma, V.: Synergistic and Antagonistic Interactions among the Particulate Matter Components in Generating Reactive Oxygen Species Based on the Dithiothreitol Assay, *Environ. Sci. Technol.*, 52, 2261-2270, <https://doi.org/10.1021/acs.est.7b04261>, 2018.
- 675 Yu, Q., Chen, J., Qin, W. H., Ahmad, M., Zhang, Y. P., Sun, Y. W., Xin, K., and Ai, J.: Oxidative potential associated with water-soluble components of PM<sub>2.5</sub> in Beijing: The important role of anthropogenic organic aerosols, *J. Hazard. Mater.*, 433, 12, <https://doi.org/10.1016/j.jhazmat.2022.128839>, 2022.
- Zhang, X. J., Wang, Y. D., Yao, K. X., Zheng, H., and Guo, H. B.: Oxidative potential, environmentally persistent free radicals and reactive oxygen species of size-resolved ambient particles near highways, *Environ. Pollut.*, 341, 122858, <https://doi.org/10.1016/j.envpol.2023.122858>, 2024.
- 680 Zhao, S., Miao, D., Zhu, K. C., Tao, K. L., Wang, C. Y., Sharma, V. K., and Jia, H. Z.: Interaction of benzo [a] pyrene with Cu(II)-montmorillonite: Generation and toxicity of environmentally persistent free radicals and reactive oxygen species, *Environ. Int.*, 129, 154-163, <https://doi.org/10.1016/j.envint.2019.05.037>, 2019a.
- 685 Zhao, S., Gao, P., Miao, D., Wu, L., Qian, Y. J., Chen, S. P., Sharma, V. K., and Jia, H. Z.: Formation and Evolution of Solvent-Extracted and Nonextractable Environmentally Persistent Free Radicals in Fly Ash of Municipal Solid Waste Incinerators, *Environ. Sci. Technol.*, 53, 10120-10130, <https://doi.org/10.1021/acs.est.9b03453>, 2019b.
- Zhong, H., Huang, R.-J., Lin, C., Xu, W., Duan, J., Gu, Y., Huang, W., Ni, H., Zhu, C., and You, Y.: Measurement report: On the contribution of long-distance transport to the secondary aerosol formation and aging, *Atmos. Chem. Phys.*, 22, 9513-9524, <https://doi.org/10.5194/acp-22-9513-2022>, 2022.
- 690